Nuclear Structure Information from the (p,t) Reaction, $A=46$ to $A=70$†

G. BASSANI,‡ NORTON M. HINTZ, AND C. D. KAVALOSKI*
School of Physics, University of Minnesota, Minneapolis, Minnesota
(Received 25 May 1964)

The (p,t) reaction has been studied with 40-MeV protons for a sequence of isotopes from titanium to zinc. Angular distributions have been obtained for ground-state ($L=0$) and first-excited-state, or lowest $L=2$ group, transitions. The shapes of the angular distributions are nearly identical for a given angular-momentum transfer L. The reaction seems to proceed by the direct pickup of a neutron pair coupled to angular momentum L. Energy spectra of the outgoing tritons were obtained for some of the elements, showing that the predominant strength goes to the lowest $L=0$ (usually the ground state) and $L=2$ transitions. The general features of the (p,t) reaction are discussed, showing that the reaction is a powerful tool for studying the angular-momentum coupling of pairs and pair correlation effects. A sketch of the distorted-wave Born-approximation (DWBA) theory for two-nucleon transfer reactions is presented together with a discussion of the spectroscopic factors predicted by neutron seniority, pairing theory, the degenerate model, and exact shell-model calculations within a pure $f_{7/2}$ configuration. Since reliable DWBA calculations are not available, we have compared our integrated cross sections with spectroscopic factors predicted by the various models. The agreement is very good for the $L=0$ transitions in the $f_{7/2}$ shell. Appreciable configuration mixing is evident in the $2p-1f_{5/2}$ shell, where both the degenerate model and pairing theory are in qualitative agreement with the data, predicting however too rapid a rise with increasing neutron number for the nickel isotopes. The behavior of the lowest $L=2$ transitions in the $2p-1f_{5/2}$ shell indicates that the first $2+$ states are not very pure in neutron seniority. Reliable DWBA calculations, including finite-range effects, are needed to remove uncertainties in the intepretation of the data.

I. INTRODUCTION

THE (p,t) reaction offers certain unique features for the study of nuclear energy levels and coupling schemes. Because of its high negative Q value (generally -5 to -15 MeV) and relatively low cross section only a few experiments have been published.[1–6] These previous experiments showed that at energies $\gtrsim 20$ MeV the process is a direct interaction, in which a neutron pair is picked up to form a triton. Although there is little direct evidence, knockout and exchange processes are probably unimportant, at least for heavy nuclei and at forward angles.

The (p,t) reaction can be expected to give the following information relating to nuclear structure: (a) Location of energy levels in otherwise inaccessible nuclei such as Ca^{38}, Fe^{52}, Ni^{56}, etc. (b) The total orbital angular momentum L to which the picked up pair is coupled will be revealed by the angular distribution. In addition, $L=J$, where J is the total angular momentum of the pair in the (p,t) reaction. In the case of even-even target nuclei, this will lead to a unique determination of the angular momentum of the final state of the residual nucleus. (c) The intensities of various groups in the triton spectra will give the distribution of "single-pair" strength in the residual nucleus, in a manner analogous to the way in which the location of the single particle strength is given by one nucleon transfer cross sections. (d) If a complete two-nucleon transfer reaction theory can be developed, which includes finite-range two-body forces and finite triton size effects, the cross sections will give information about the spatial and momentum correlation of neutron pairs in the target ground state. This sensitivity to pair correlation effects has no analog in single-neutron transfer reactions. To obtain this last kind of information it will be necessary to estimate the relative importance of single-step processes in which the pickup occurs when both neutrons lie within the range of a triton and two-step processes in which a (p,d) followed by a (d,t) reaction occur at different points in the nucleus. (e) The pair pickup reaction will give information on the relative phases (occupation amplitudes) of nucleons occupying various orbital states pairwise, rather than simply the individual occupation probabilities as in single-nucleon transfer reactions.

Because of the interesting information to be obtained from (p,t) reactions, it was decided to study a series of nuclei in the $1f-2p$ shell where targets are readily available and considerable theoretical work has been done.

In Sec. II we discuss the selection rules to be expected for (p,t) reactions, in Secs. III and IV the experimental methods and results, and in Sec. V the theory. In Sec. VI we present a discussion of the relative spectroscopic factors observed in the experiment and in Sec. VII our conclusions.

† Work supported in part by the U. S. Atomic Energy Commission.

‡ Present address: C. E. N. Saclay, France.

* Present address: Department of Physics, University of Washington, Seattle, Washington.

[1] J. B. Ball and C. D. Goodman, Phys. Rev. **120**, 488 (1960).

[2] G. Bassani, C. D. Kavaloski, and N. M. Hintz, *Direct Interactions and Nuclear Reaction Mechanisms* (Gordon and Breach Science Publishers, New York, 1963), p. 517.

[3] C. D. Goodman, J. B. Ball, and C. B. Fulmer, *Direct Interactions and Nuclear Reaction Mechanisms* (Gordon and Breach Science Publishers, New York, 1963), p. 527.

[4] J. C. Legg, Phys. Rev. **129**, 272 (1963).

[5] J. B. Ball, C. B. Fulmer, and C. D. Goodman, Phys. Rev. **130**, 2342 (1963).

[6] H. D. Holmgren and C. B. Fulmer, Phys. Rev. **132**, 2644 (1963).

II. SELECTION RULES

In order to facilitate presentation of the experimental data we give a brief discussion of the selection rules[7] expected for the (p,t) reaction.

We denote the initial and final nuclear total angular momenta by $\mathbf{J}_i$ and $\mathbf{J}_f$. The two transferred neutrons are assumed to have individual orbital, intrinsic, and total angular momenta in the target nucleus, $\mathbf{l}_1$, $\mathbf{l}_2$; $\mathbf{s}_1$, $\mathbf{s}_2$; and $\mathbf{j}_1$, $\mathbf{j}_2$. In addition the pair is assumed to be coupled to a total angular momentum $\mathbf{J}$, with total orbital and spin angular momenta, $\mathbf{J}$ and $\mathbf{S}$. The orbital angular momenta are measured relative to the center of mass of the target nucleus. The total orbital angular momentum of the neutron pair, $\mathbf{L}$, can also be decomposed into a sum of the angular momentum of the center of mass of the pair, $\mathbf{\Lambda}$, and the relative angular momentum of the pair, $\boldsymbol{\lambda}$. Then $\mathbf{L}=\mathbf{l}_1+\mathbf{l}_2=\mathbf{\Lambda}+\boldsymbol{\lambda}$, and $\mathbf{S}=\mathbf{s}_1+\mathbf{s}_2$.

Certain selection rules are exact, for a single-step direct two-neutron pickup reaction, while others are only approximate. We list them in order of decreasing strength. The following two selection rules are exact:

$$|J_i-J_f|\leq J\leq(J_i+J_f) \tag{1}$$

and

$$\Delta\pi=(-1)^{l_1+l_2}=(-1)^{\Lambda+\lambda}, \tag{2}$$

where $\Delta\pi$ is the parity change between the initial and final nuclear states. The second selection rule implies that if the two neutrons are picked up from the same shell $\Delta\pi=+1$. In addition, if $(l_1j_1)=(l_2j_2)$ for the two neutrons, the Pauli principle restricts J to even values.

The following selection rules are approximate and are based on the fact that the two neutrons in the triton are in a relative space symmetric ($\lambda=$even), $S=0$ state approximately 95% of the time[8] and therefore $J=L$:

$$|J_i-J_f|\leq L\leq(J_i+J_f) \tag{3}$$

and

$$\Delta\pi=(-1)^{\Lambda}. \tag{4}$$

The total angular-momentum change in the reaction J is then just the orbital angular momentum of the transferred pair L. In the case of an even-even target nucleus rule (3) reduces to $J_f=L$. It will be seen below that the angular distributions generally give a unique determination of L and hence of J_f for an even-even nucleus.

Selection rule (4) arises because for identical nucleons λ must be even when $S=0$. This selection rule might inhibit certain transitions allowed by (2).

The following selection rule is somewhat weaker than (3) and (4) and would hold if the triton wave function contained only relative s-state motion between the neutrons ($\lambda=0$). For example, a wave function of the form

$$\psi=A\sum_{i>j}\exp[-\alpha(\mathbf{r}_{ij})^2],$$

where $\mathbf{r}_{ij}$ is the relative coordinate of any two nucleons, would satisfy this condition. The point triton assumption sometimes made is a special case of the above wave function with $\alpha\rightarrow\infty$. In case $\lambda=0$. the parity rule (2) reduces to

$$\Delta\pi=(-1)^L=(-1)^J. \tag{5}$$

Taken together with rule (3) selection rule (5) implies that for even-even targets only natural parity states can be excited. If an unnatural parity state is observed, a determination of the L value through a measurement of the angular distribution should indicate whether selection rule (3) or (5) is being violated.

Finally, there are isotopic spin and seniority selection rules which are exact. The isotopic spin selection rule is

$$|T_i-T_f|\leq 1\leq(T_i+T_f), \tag{6}$$

where T_i and T_f are the initial and final total isotopic spins of the nuclear states. This selection rule arises because the isotopic spin of the transferred neutron pair is unity. The seniority selection rule is

$$\Delta\nu_n=0,\pm 2, \tag{7}$$

where ν_n is the neutron seniority. This selection rule arises from the fact that we are, at most, breaking two neutron pairs in a direct (p,t) reaction.

The above selection rules, (1) through (7), are still valid if the (p,t) reaction occurs in two steps as mentioned above. It should also be emphasized that although quantities such as J, L, Λ, T_i, T_f, and ν_n may not be good quantum numbers for the states involved, the (p,t) reaction can nevertheless proceed only through those components of the wave functions which satisfy the above selection rules. Finally, it is assumed in the direct (p,t) reaction that the proton configuration remains unchanged. The selection rules are, of course, valid for (n,He^3) reactions if we exchange neutron with proton in the wording above.

III. EXPERIMENTAL METHODS

The experiments were performed using the 39.8 ± 0.2 MeV beam of the University of Minnesota linear accelerator. The tritons were selected by a 40-in., 180° magnetic spectrometer and a detector array of eight $\frac{1}{16}$-in.-thick plastic scintillators in the focal plane of the spectrometer. The outputs of each of the eight detectors were analyzed using a Nuclear Data-101, 256-channel pulse-height analyzer, split into eight 32-channel subunits in a manner described in a previous paper.[9] The energy resolution of the system, which was $\sim$1.5%, was

[7] We are indebted to Professor Ben Bayman for much of the following discussion on selection rules. These selection rules have also been discussed by N. K. Glendenning, Nucl. Phys. **29**, 109 (1960), and H. C. Newns (Ref. 26).

[8] J. M. Blatt, G. H. Derrick, and J. N. Lyness, Phys. Rev. Letters **8**, 323 (1962).

[9] C. D. Kavaloski, G. Bassani, and N. M. Hintz, Phys. Rev. **132**, 813 (1963).

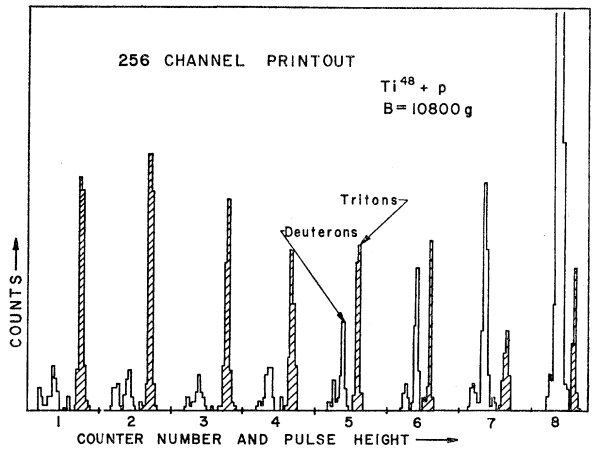

FIG. 1. Printout of the 256-channel analyzer in a region where deuteron and triton spectra are overlapping. Due to their different pulse height, deuterons and tritons can be easily separated in each counter.

determined mainly by the height of the counters (0.8-in.) and the energy spread of the linac beam.

Since the tritons generally had the highest magnetic rigidity, no difficulty was encountered in particle identification for the ground-state group and for the first few MeV of excitation. However, at higher excitation, deuterons occurred at the same magnetic rigidity and had to be eliminated by pulse-height selection in the counters. This was sometimes difficult since the scintillator thickness had been selected for (p,d) experiments and was not optimum for triton-deuteron separation. Figure 1 shows a printout of the 256-channel analyzer showing deuteron and triton peaks in the eight counters.

Since the deuteron yields were much higher than the triton, the data presented here generally stop at a magnetic rigidity corresponding to the ground state deuterons.

The beam current was monitored by a small Faraday cup (of unknown efficiency) inside the 12-in. Mylar windowed target chamber. The counting rate was kept low enough to keep losses due to the dead time of the analyzer (about 85 μsec) below 2%. The dead time losses were monitored in the early runs by looking at the spectrum from a single counter with a fast (2 μsec) transistorized 22-channel analyzer. Data taken at different times were normalized to the cross section at 20° (lab) for $Fe^{56}(p,t)Fe^{54}$, ground state, measured with a standard target, to insure good relative accuracy of cross sections ($\sim\pm10\%$). Absolute cross sections were obtained by measuring known elastic-proton cross sections at 40 MeV and from foil weights and are estimated to be good to $\pm20\%$.

The targets used in this experiment were Ti^{46}, Ti^{48}, Ti^{50}, V^{51}, Cr^{52}, Mn^{55}, Fe^{54}, Fe^{56}, Fe^{58}, Co^{59}, Ni^{58}, Ni^{60}, Ni^{62}, Ni^{64}, Cu^{63}, Cu^{65}, Zn^{64}, Zn^{66}, Zn^{68}, and Zn^{70}. The V^{51}, Cr^{52}, and Co^{59} were natural isotopic foils. The Mn^{55} was prepared by evaporation on an aluminum backing 2.0 mg/cm². The remaining targets were procured from the Isotope Sales Division, Oak Ridge National Laboratory. The target thicknesses and enrichments are given in Table I.

TABLE I. List of areal densities, enrichments, and (p,t) ground-state Q values for the elements studied. The enrichments are from the Oak Ridge National Laboratory mass analysis supplied with the enriched isotopes. In the case of V^{51}, Cr^{52}, Mn^{55}, and Co^{59} natural targets have been used. The Q values are taken from Ref. 10 except for Ni^{58}. The value quoted for this element has been taken from Ref. 15.

Element	Areal density (mg/cm²)	Enrichment (%)	Q value (MeV)
Ti^{46}	4.86	86.4	−14.124
Ti^{48}	20.99	98.86	−12.025
Ti^{50}	4.94	69.7	−10.603
V^{51}	10.55	99.76 (nat.)	−11.894
Cr^{52}	2.56	83.76 (nat.)	−12.818
Mn^{55}	9.3	100 (nat.)	−10.677
Fe^{54}	4.93	97.21	−15.578
Fe^{56}	49.84	99.70	−12.028
Fe^{58}	1.3	78.4	−9.207
Co^{59}	15.18	100 (nat.)	−10.284
Ni^{58}	8.0	≥99.0	−13.970
Ni^{60}	25.71	99.83	−11.907
Ni^{62}	5.03	98.7	−9.931
Ni^{64}	5.05	99.81	−8.020
Cu^{63}	37.48	99.85	−11.247
Cu^{65}	49.71	98.16	−9.344
Zn^{64}	4.67	99.85	−12.535
Zn^{66}	3.85	97.8	−10.545
Zn^{68}	4.50	99.3	−8.762
Zn^{70}	5.21	78.3	−7.211

In the areal density measurements, a contact print of the target was enlarged several times and then measured with a planimeter. Although the errors in the measured areal densities were less than $\pm0.5\%$, a larger error ($\pm5\%$) was assumed in the calculation of the cross sections due to uncertainties in target uniformity. This method could not be used for the foils Mn^{55}, Fe^{58}, and Ni^{58}. These thicknesses were measured in scattering experiments, making use of known cross sections. The error in the areal density for these cases is then assumed to be $\pm10\%$.

Data were generally taken at 5-deg intervals between 7° and 40 to 60°. The lower limit was determined by the

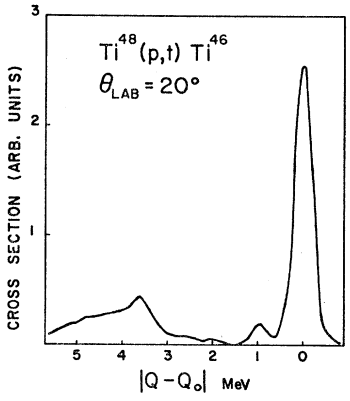

FIG. 2. Energy spectrum of tritons from $Ti^{48}(p,t)Ti^{46}$.

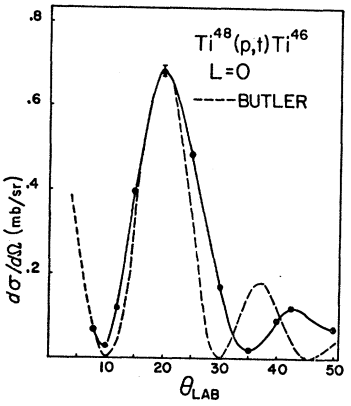

FIG. 3. Angular distribution of tritons from $Ti^{48}(p,t)Ti^{46}$, ground state. The dashed line represents a plane wave Butler fit obtained with a radius $r=8.63$ F.

size of the Faraday cup while the upper limit was set by intensity considerations. This angular range gave sufficient information to determine the L value of the transition and to cover the principal maxima in the cross section.

Energy spectra were taken by changing the spectrometer field so as to shift the spectra by five or six counters to achieve some overlap in the data. Linearity between the field and momentum was checked using reactions with known Q values so as to establish the energy scale.

IV. RESULTS

A. General

The energy spectra and angular distributions obtained in this experiment are shown in Figs. 2 through 27. The error bars on the angular distributions indicate statistical errors only. The ordinate in the energy spectra is proportional to the number of counts per unit charge in each counter, that is, to $d\sigma/d\omega dx$, where dx is the width of one counter in the focal plane.

Whenever possible we have used known Q values[10] to establish energy scales, otherwise relative Q-values obtained from our field and position measurements are good to ± 150 keV unless otherwise indicated. All of the data are presented in the laboratory coordinate system.

In general, only the first strong $L=0$ and $L=2$ transitions were clearly resolved. The lowest $L=0$ transition (generally to the ground state) was strongest, and all $L=0$ transitions studied had very similar angular distributions, with minima and maxima at the same angle to within about one degree, despite the range of Q values and mass numbers studied. The $L=2$ shapes fluctuate somewhat but are out of phase with the $L=0$ and so are quite easy to recognize. A sufficient number of known $L=0$ and $L=2$ transitions [selection rules(3)] were observed so that identification of unknown transitions was unambiguous for these angular momentum transfers. Integrated cross sections for the transitions studied are given in Table II.

[10] The Q values used in this work were taken from the U. S. Atomic Energy Commission 1960 Nuclear Data Tables (unpublished); the energies and spins of known excited states were taken from *Landolt-Bornstein Tables*, edited by K. H. Hellwege (Springer-Verlag, Berlin, 1961), Vol. I, unless otherwise indicated.

TABLE II. Integrated cross sections for the $L=0$ ground state and the lowest $L=2$ transitions for the elements studied. The excitation energies of the $L=2$ transitions are listed in the third column. The numbers in parenthesis refer to the center of gravity of the $L=2$ triton groups which are known to include several levels. The excitation energies of the first 2+ states in Ti^{44} and Zn^{62} are at present not available. The value listed in the $L=0$ column for Mn^{55} represents the sum of the ground-state transition (probably $L=2$) and the first excited state transition (probably $L=0$). The figure quoted in parenthesis for Mn^{55} is the integrated $L=0$ cross section obtained by subtracting an estimate of the $L=2$ cross section made from the shape of the angular distribution.

Target nucleus	$L=0$	$L=2$	$L=2$ Excitation energy (MeV)
Ti^{46}	5.43	0.93	
Ti^{48}	6.27	1.03	0.89
Ti^{50}	3.86	2.04	0.99
V^{51}	3.36	1.29	(1.00)
Cr^{52}	4.12		
Mn^{55}	5.96 (3.8±0.8)		
Fe^{54}	3.12	1.15	0.85±0.05
Fe^{56}	5.41	0.65	1.41
Fe^{58}	6.13		
Co^{59}	7.18	2.73	(1.70)
Ni^{58}	6.35	1.08	(2.85±0.15)
Ni^{60}	8.56	1.96	1.45
Ni^{62}	8.88	3.04	1.33
Ni^{64}	8.00	3.72	1.17
Cu^{63}	7.14		
Cu^{65}	6.03		
Zn^{64}	8.14	1.56	
Zn^{66}	8.27	2.20	0.99
Zn^{68}	7.55	2.46	1.04
Zn^{70}	6.46	2.04	1.08

We now discuss the individual spectra and angular distributions.

B. $Ti^{48}(p,t)Ti^{46}$

The spectrum (Fig. 2) is dominated by the strong ground state $L=0$ transition (Fig. 3). This seems to be a general feature of (p,t) reactions for the even-even nuclei studied in this experiment. The known 2+ state at 0.887 MeV provides us with an $L=2$ angular distribution (Fig. 4). The $L=4$ transition to the 4+ state at 2.006 MeV is very weak but considerable strength is observed in a group of unresolved state about 3-MeV ex-

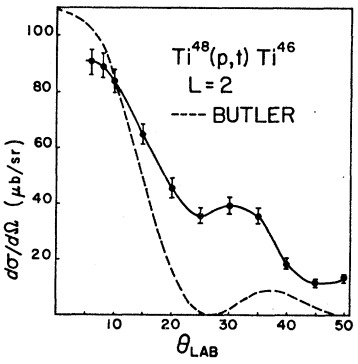

FIG. 4. Angular distribution of tritons from $Ti^{48}(p,t)Ti^{46}$, 0.887-MeV state. The dashed line represents a plane-wave Butler fit obtained with a radius $r=5.0$ F. Using the same radius as for the $L=0$ ground state fit, the second maximum occurs at 19°.

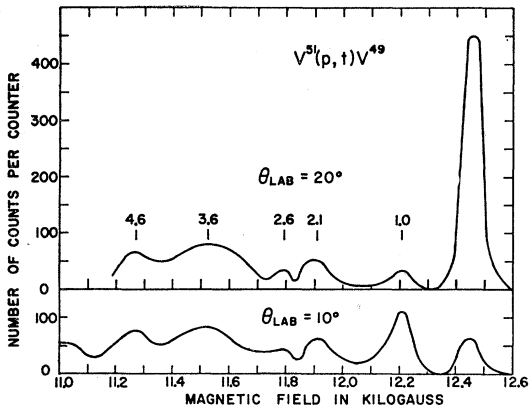

FIG. 5. Energy spectra of tritons from $V^{51}(p,t)V^{49}$.

citation. These observations are in qualitative agreement with shell-model calculations on $f_{7/2}$ nuclei by Bayman *et al.*, which will be discussed in Secs. VC4 and VIA.

A search was made for a possible backward peak in the $Ti^{48}(p,t)Ti^{46}$ ground-state angular distribution due to contributions from heavy-particle stripping or exchange effects, but no appreciable cross section could be seen from 75 to 140°.

C. $V^{51}(p,t)V^{49}$

Energy spectra for V^{51} were taken at 10 and 20° (Fig. 5) which are the maxima in the $L=2$ and $L=0$

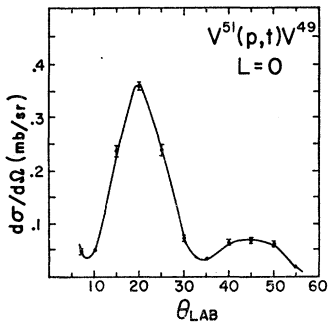

FIG. 6. Angular distribution of tritons from $V^{51}(p,t)V^{49}$, ground state, 0.089- and 0.15-MeV states.

angular distributions, respectively. These spectra then reveal any well resolved $L=0$ or 2 transitions. Angular distributions were taken on the ground-state group (Fig. 6) and the group at 1.0 MeV (Fig. 7). These showed relatively pure $L=0$ and $L=2$ shapes as can be seen by comparison with Figs. 3 and 4.

Since the ground-state spins and parities of V^{51} and V^{49} are both $\frac{7}{2}-$, selection rule (3) allows $L=0,1,2,\cdots 7$. Selection rule (5), however, should restrict L to even values, as would also be the case if both picked-up neutrons were in the same shell. However, from the deep minimum at ~8° in the ground-state angular distribution it can be concluded that more than 90% of the cross section comes from the $L=0$ contribution. This is also in agreement with Bayman's results [Secs. VC4 and VIA showing weak $L=2$, 4, and 6 spectroscopic factors for this state. In addition, because of our resolution (~350 keV), the state in V^{49} at 89 keV (probably $\frac{5}{2}-$) and 150 keV (probably $\frac{3}{2}-$) would be included in our "ground-state" peak and these would require $L\geq 2$. Thus we can place an upper limit for the cross section to these states at $\lesssim 10\%$ of the ground-state cross section.

The group at 1.0 MeV shows a pure $L=2$ transition (although a small amount of $L=4$ cannot be excluded), and occurs at approximately the same excitation energy as the 2+ states in neighboring even nuclei, as would be expected from a simple core excitation model. Several states, or unresolved groups, are seen at higher excita-

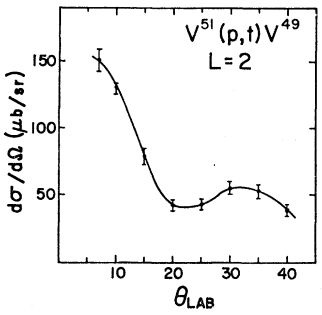

FIG. 7. Angular distribution of the 1.0-MeV triton group from $V^{51}(p,t)V^{49}$.

tion energy (2.1, 2.6, 3.6 and 4.6 MeV) but no strong $L=0$ or $L=2$ groups are observed. Peaks which show no strong angular dependence between 10 and 20° could either be $L=4$ or higher [see Sec. IVH] or a mixture of $L=0$ and $L=2$.

D. $Mn^{55}(p,t)Mn^{53}$

Figure 8 shows the spectrum for this reaction, taken at 15°. The strong peak near zero excitation energy shows a predominately $L=0$ shape (Fig. 9), but contains a significant $L=2$ contribution, as can be seen from

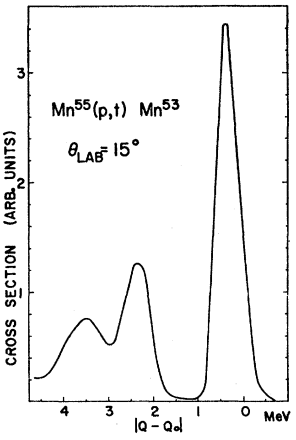

FIG. 8. Energy spectrum of tritons from $Mn^{55}(p,t)Mn^{53}$.

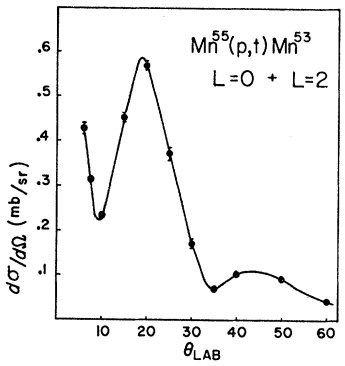

FIG. 9. Angular distribution of tritons from $Mn^{55}(p,t)Mn^{53}$, ground state and 0.37 MeV state.

the filling in of the minimum at 10°. Since the ground-state spin of Mn^{55} is $\frac{5}{2}-$ and that of Mn^{53} is $\frac{7}{2}-$, the ground-state transition must go by $L\geq 2$. However, there is a low state (0.37 MeV) in Mn^{53} which we cannot resolve from the ground state. We can conclude from the $L=0$ shape and selection rules (3) and (5) that this state must have spin and parity $\frac{5}{2}-$. This is in disagreement with an earlier work[11] which made an assignment of $\frac{3}{2}-$ for this state. The $L=2$ component of the strong group could come from an $L=2$ contribution to the $\frac{5}{2}-$ state, which is allowed by the selection rules. However, it is more likely to be from an $L=2$ excitation of the $\frac{7}{2}-$ ground state, since we have found in other

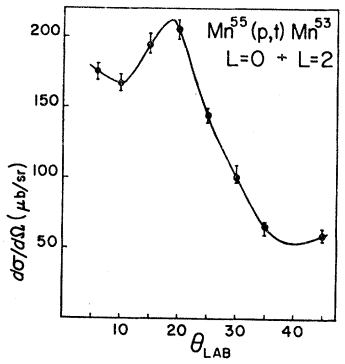

FIG. 10. Angular distribution of the 2.3-MeV triton group from Mn^{55}-$(p,t)Mn^{53}$.

cases (V^{51}, Co^{59}, Cu^{63}, Cu^{65}) where the selection rules allow $L=2$ as well as $L=0$, that a pure $L=0$ shape is seen.

The $L=0$ strength seen for the $\frac{5}{2}$- to $\frac{5}{2}$-transition in $Mn^{55}(p,t)Mn^{53}$ is comparable to that seen in neighboring even nuclei (see Table II). This is in strong disagreement with a recent shell-model calculation by Schwarcz[12] in which the two valence neutrons in Mn^{55} are found to be predominately in the configuration $(p_{3/2})(f_{5/2})$ coupled to $J=1$ in order to explain the anomalous ground-state spin. An $L=0$ shape could only be observed for pickup of a $J=1$ neutron pair if $S=1$, which is $\sim 95\%$ forbidden for the (p,t) reaction (see Sec. II).

[11] G. Bassani, L. Colli, E. Gadioli, and I. Iori, Nucl. Phys. **36**, 471 (1962).
[12] E. H. Schwarcz, Phys. Rev. **129**, 727 (1963).

The triton group at 2.3-MeV excitation shows a mixture of $L=0$ and $L=2$, or possibly other L values (Fig. 10), while the group at 3.5 MeV seems to be mainly $L=2$ (Fig. 11).

It should be pointed out that, unlike the situation for V^{51} and Co^{59} [Sec. IVG], the dominant $L=2$ strength does not appear near an excitation energy corresponding to the 2+ states in the neighboring even nuclei as would be expected on a core-excitation model. High resolution data on the (p,t) reaction for Mn^{55} would be highly desirable.

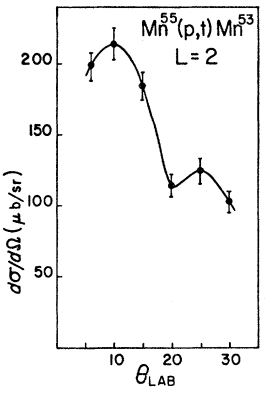

FIG. 11. Angular distribution of the 3.5-MeV triton group from $Mn^{55}(p,t)Mn^{53}$.

E. $Fe^{54}(p,t)Fe^{52}$

By using a thinner target, the broad group reported earlier[2] was seen to consist of an $L=0$ ground state and a clearly resolved $L=2$ transition to a 2+ state at 0.85 ± 0.05 MeV, which has not been previously reported. The $L=0$ and $L=2$ angular distributions showed the standard shapes. Spectra are not yet available. Integrated cross sections for the $L=0$ and $L=2$ transitions are shown in Table II.

F. $Fe^{56}(p,t)Fe^{54}$

As in the case of Fe^{54}, use of a thinner target enabled the 2+ state at 1.41 MeV to be resolved from the

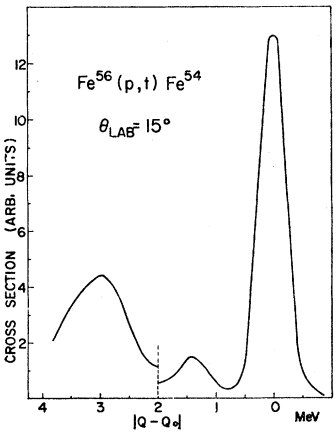

FIG. 12. Energy spectrum of tritons from $Fe^{56}(p,t)Fe^{54}$. The part of the spectrum up to 2 MeV of excitation was taken with a natural Fe foil 20 mg/cm² thick. In order to avoid the interference from the reaction $Fe^{54}(p,t)Fe^{52}$, the rest of the spectrum was taken with a much thicker enriched target, listed in Table I.

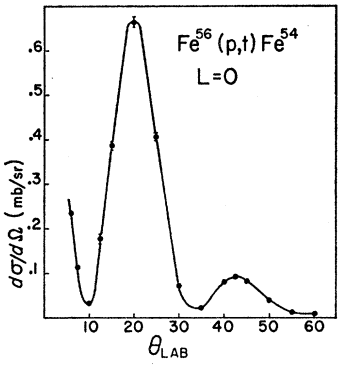

FIG. 13. Angular distribution of tritons from $Fe^{56}(p,t)Fe^{54}$, ground state.

ground state and higher states (Fig. 12). The ground state and 2+ state showed again the standard $L=0$ and $L=2$ shapes (Figs. 13 and 14). The broad group at 3 MeV contains at least three states.[13] An angular distribution was not made for this state due to insufficient resolution.

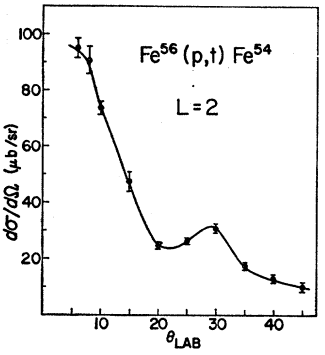

FIG. 14. Angular distribution of tritons from $Fe^{56}(p,t)Fe^{54}$, 1.41-MeV state.

G. $Co^{59}(p,t)Co^{57}$

The spectra at 10 and 20° are shown in Fig. 15. As is generally the case for the odd-Z nuclei, the ground-state

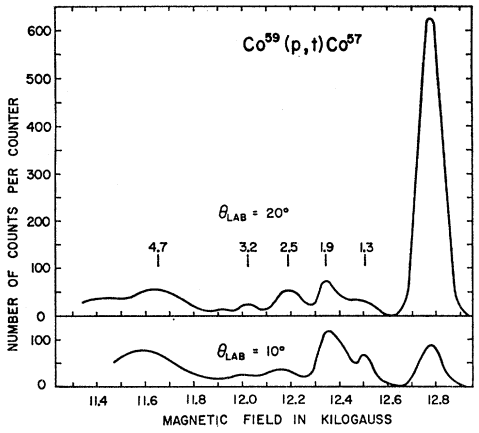

FIG. 15. Energy spectra of tritons from $Co^{59}(p,t)Co^{57}$.

[13] R. Sherr (private communication).

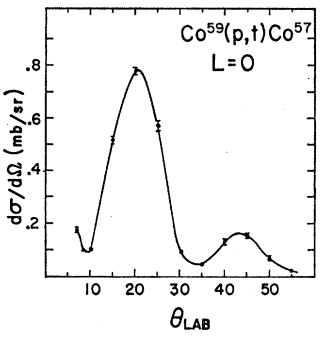

FIG. 16. Angular distribution of tritons from $Co^{59}(p,t)Co^{57}$, ground state.

transition shows a pure $L=0$ transition (Fig. 16), despite the fact that the selection rules allow higher values. Figure 17 shows the angular distribution for the combined peak at 1.3 and 1.9 MeV, probably corresponding to the known states at 1.37 and 1.90 MeV.

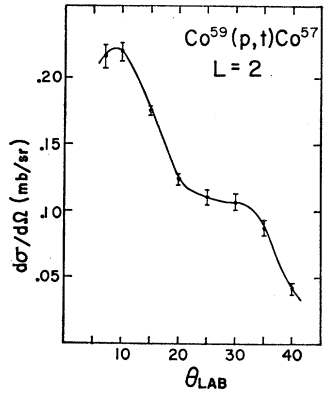

FIG. 17. Angular distribution of tritons from $Co^{59}(p,t)Co^{57}$ corresponding to states from 0.9 to 2.1 MeV of excitation. The two main triton groups observed are at 1.3 and 1.9 MeV (Fig. 15).

This angular distribution seems to have a relatively pure $L=2$ shape, although we cannot exclude a small $L=4$ contribution from the above states or the state at 1.49 MeV ($\frac{1}{2}-$) which requires $L=4$. The center of gravity of this $L=2$ group is at 1.6 to 1.7 MeV, slightly higher than the neighboring 2+ state energies.

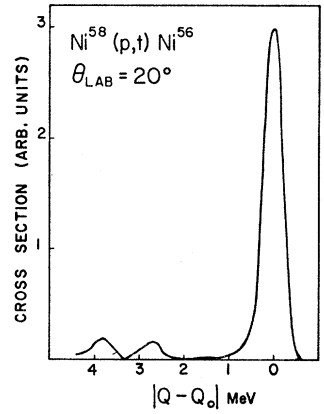

FIG. 18. Energy spectrum of tritons from $Ni^{58}(p,t)Ni^{56}$.

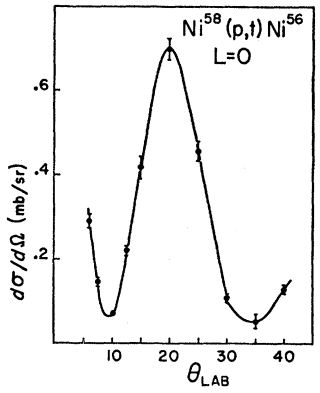

FIG. 19. Angular distribution of tritons from $Ni^{58}(p,t)Ni^{56}$, ground state.

H. $Ni^{58}(p,t)Ni^{56}$

This reaction is especially interesting because it leads to doubly magic Ni^{56}. The Ni^{58} (p,t) spectrum (Fig. 18) shows a strong ground-state peak and peak due to states not previously reported at 2.85 ± 0.15 and 3.87 ± 0.15 MeV. The measured ground state Q value,

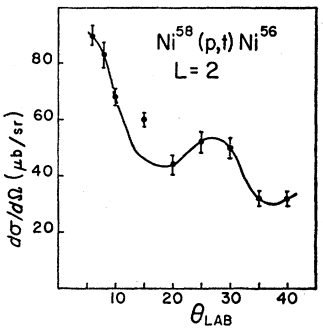

FIG. 20. Angular distribution of the 2.85-MeV triton group from $Ni^{58}(p,t)Ni^{56}$.

-13.8 ± 0.2 MeV, is in good agreement with a calculation[14] of the total binding energy of Ni^{56} which lead to a theoretical Q value of -13.65 MeV. The Q value reported here supersedes the value published earlier.[2] Recently, the Colorado group[15] has studied this reac-

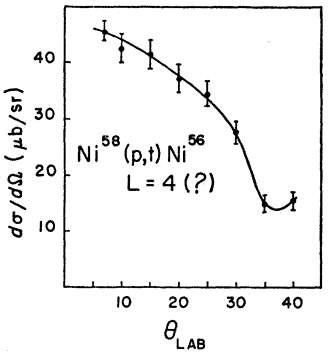

FIG. 21. Angular distribution of the 3.87-MeV triton group from $Ni^{58}(p,t)Ni^{56}$.

[14] I. Talmi, Rev. Mod. Phys. 34, 704 (1962).
[15] C. Hoot, M. Kondo, and M. Rickey, Bull. Am. Phys. Soc. 8, 598 (1963).

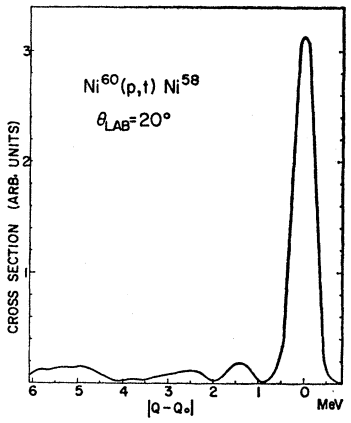

FIG. 22. Energy spectrum of tritons from $Ni^{60}(p,t)Ni^{58}$.

tion and found a ground state Q value of -13.970 ± 0.017 MeV and evidence for three states[15a] at 2.41, 2.71, and 3.12 MeV. which may correspond to our 2.85-MeV group. They also observe a group 3.97 MeV which

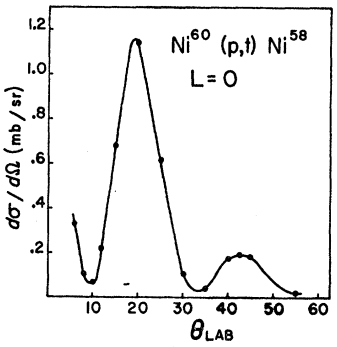

FIG. 23. Angular distribution of tritons from $Ni^{60}(p,t)Ni^{58}$, ground state.

probably corresponds to the peak we observe at 3.87 MeV.

The ground state shows a pure $L=0$ (Fig. 19) shape while the 2.85 MeV group shows the $L=2$ shape (Fig.

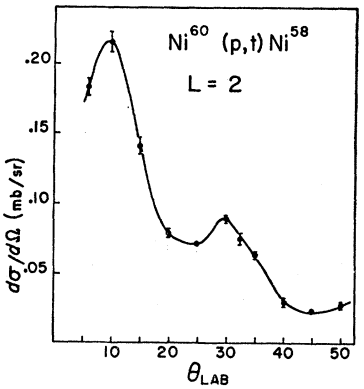

FIG. 24. Angular distribution of tritons from $Ni^{60}(p,t)Ni^{58}$, 1.452-MeV state.

[15a] *Note added in proof*. Later work by Hoot *et al.* shows only a single state in this region at 2.71 ± 0.05 MeV, which they assign $J,\pi=2+$ or $4+$. They believe the higher state, which they observe at 3.94 ± 0.05 MeV to be $J,\pi=0+$ (C. Hoot, private communication).

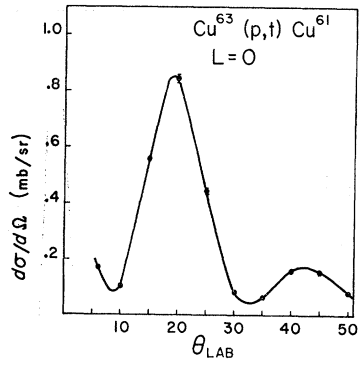

FIG. 25. Angular distribution of tritons from $Cu^{63}(p,t)Cu^{61}$, ground state.

20). The errors are somewhat larger for the angular distribution of the 3.87-MeV group (Fig. 21) since the tritons were near the ground state deuteron group in magnetic rigidity. However, the angular distribution is very similar (allowing for a scale shift due to the energy change) to that found by Ball *et al.*,[5] for a known 4+ state in Fe^{56} from the reaction Fe^{58} (p,t) Fe^{56} at $E_p=22$ MeV; so we tentatively assign $J,\pi=4+$ to this state.

Ni^{56} is unusual for a doubly closed shell nucleus in that states of the same parity as the ground state can be formed by single particle-hole excitations across one shell. The relatively strong excitation of the 2+ state in Ni^{56} seems to be evidence against a configuration of a doubly closed $1f_{7/2}$ shell plus two neutrons in the $1f_{5/2}-2p$ shell for the ground state of Ni^{58}. With this configuration, removal of the two $f-p$ neutrons would lead uniquely to the ground state of Ni^{56}, while removal of two neutrons from the $f_{7/2}$ shell should lead to states of fairly high excitation in Ni^{56} since the separation between the $f_{7/2}$ and $2p_{3/2}-f_{5/2}$ shells is believed to be about 5 MeV.[16] The 2+ state could be excited, assuming the above configuration for Ni^{58}, by removing one neutron from the $f_{7/2}$ shell and one from the $2p-f_{5/2}$ shell. The cross section for this process should, however,

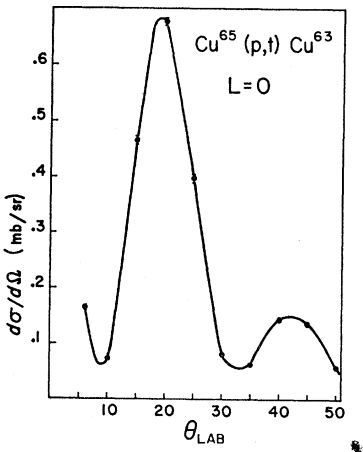

FIG. 26. Angular distribution of tritons from $Cu^{65}(p,t)Cu^{63}$, ground state.

[16] B. L. Cohen, R. H. Fulmer, A. L. McCarthy, and P. Mukerjee, Rev. Mod. Phys. **35**, 332 (1963).

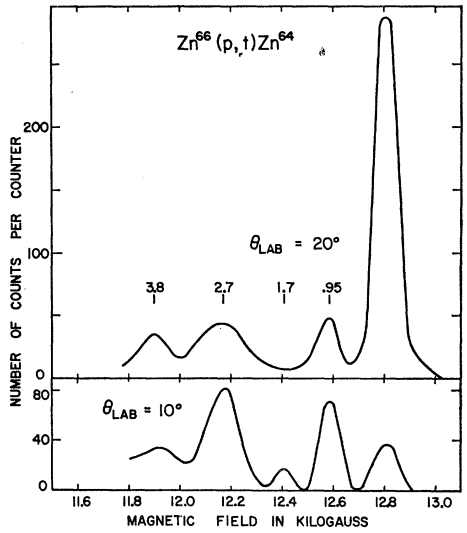

FIG. 27. Energy spectra of tritons from $Zn^{66}(p,t)Zn^{64}$.

be considerably reduced by angular momentum recoupling factors and the radial overlap integral involving the f and p orbitals. One explanation of the strong 2+ excitation would be to assume a component in the Ni^{58} ground state in which four neutrons occupy the $f_{5/2}-2p$ shell as would be expected from quadrupole correlations or "vibrations" in the ground state.[17] Pickup of one pair could then leave the remaining pair coupled to 2+ (or 4+).

I. $Ni^{60}(p,t)Ni^{58}$

The spectrum for this reaction, taken at 20°, is shown in Fig. 22. The strong ground-state group and the well resolved 2+ group at 1.45 MeV show the usual $L=0$ and $L=2$ angular distributions (Figs. 23 and 24). The group at ~2.5 MeV contains the known "two phonon" 2+ and 4+ states, which could not be resolved. No significant strength is seen at the position of the known 3− state in Ni^{58} (4.5 MeV), which is strongly excited in inelastic scattering. According to the picture of the 3− vibrational states developed by Brown and co-workers,[18] the 3− state in Ni^{58} would be formed by a coherent superposition of one-particle one-hole excitations, mainly from the $1f-2p$ shell into the $1g-2d$ shell. Since the $1g-2d$ shell is expected to have very little occupation in the ground state of Ni^{60}, these components cannot be excited in the (p,t) reaction.

J. $Cu^{63}(p,t)Cu^{61}$ and $Cu^{65}(p,t)Cu^{63}$

Only the ground-state transitions, both of which show a relatively pure $L=0$ shape (Figs. 25 and 26) have been studied for the copper isotopes. Since the ground-state spins are all $\frac{3}{2}-$, $L=0$ and 2 are permitted

[17] G. E. Brown (private communication).
[18] G. E. Brown, L. Castillejo, and J. A. Evans, Nucl. Phys. **22**, 1 (1961).

by the selection rules. Thus the situation is the same as for V^{51} and Co^{59}, indicating relatively small admixtures of 2+ core excitations in the copper ground states.

K. $Zn^{66}(p,t)Zn^{64}$

Preliminary spectra at 10 and 20° are shown in Fig. 27. The ground state and first 2+ state (0.95 MeV) showed the standard $L=0$ and $L=2$ angular distributions and are not shown here. Angular distributions for the other states are not yet available.

The spectrum of Zn^{64} has been studied recently in considerable detail by Sen Gupta and Van Patter.[19] The discussion below is based on their energy and spin assignments. The state which we see at 0.95 MeV is the known 2+ state (0.99 MeV). We do not see the 0+ states at 1.90 and 2.62 MeV. We can set an upper limit of $\lesssim 10\%$ of the ground state $L=0$ strength for these states. The weak group which we see at ~ 1.7 MeV probably corresponds to the second 2+ state at 1.804 MeV, since the ratio of the cross sections at 10 and 20° is that expected for $L=2$ transitions.

The peak at 2.7 MeV also shows about the same ratio for the cross sections at 10 and 20° as the known $L=2$ transitions. The only states in the vicinity of 2.7 MeV are states at 2.32 (4+), 2.62 (0+) and 3.00 (3−) MeV. However, since we have not seen an $L=3$ angular distribution we cannot exclude a mixture of $L=3$ and $L=4$ for this group. Further work is in progress on the Zn isotopes.

L. Ti^{46}, Ti^{50}, Cr^{52}, Fe^{58}, Ni^{62}, Ni^{64}, Zn^{64}, Zn^{68}, and Zn^{70} Targets

Work is still in progress on these nuclei. At present we have data only on the ground state ($L=0$), and in some cases first excited state ($L=2$) transitions. These nuclei all showed the standard $L=0$ and $L=2$ angular distributions. The integrated cross sections are presented in Table II and discussed in Sec. VI. Further work on these nuclei will be published later.[20]

V. THEORY, REACTION MECHANISM, AND SPECTROSCOPIC FACTORS

A. Distorted-Wave Born Approximation

The distorted-wave Born approximation (DWBA) should provide the best treatment of two-nucleon transfer reactions. The general expression for the (p,t) cross section, assuming $J=L$ for the transferred neutron pair is[21]

$$\frac{d\sigma}{d\omega}=\frac{m_i m_f}{(2\pi\hbar^2)^2}\frac{k_f}{k_i}\frac{1}{(2J_i+1)\cdot 2}\sum_{M_i M_f \mu_t \mu_p}\left|\int \phi_t^{(-)*}(\mathbf{r}_t)\Theta^*(\mathbf{r}_p,\mathbf{r}_1,\mathbf{r}_2)\chi_{\mu_t}^{1/2}(\boldsymbol{\sigma}_p)\chi_0^0(\boldsymbol{\sigma}_1,\boldsymbol{\sigma}_2)\times\psi_{M_f}^{J_f*}V(\mathbf{r}_p,\mathbf{r}_1,\mathbf{r}_2)\psi_{M_i}^{J_i}\chi_{\mu_p}^{1/2}(\boldsymbol{\sigma}_p)\phi_p^{(+)}(\mathbf{r}_p)d\tau\right|^2, \quad (8)$$

where m_i, m_f, k_i, k_f, are the initial and final reduced masses and wave numbers; J_i, M_i, J_f and M_f are the target and residual spins and projections; and μ_p, μ_t are the proton and triton spin projections.

The expressions $\phi_t^{(-)}(\mathbf{r}_t)$ and $\phi_p^{(+)}(\mathbf{r}_p)$ represent the distorted triton and proton waves; $\Theta(\mathbf{r}_p,\mathbf{r}_1,\mathbf{r}_2)$ the triton internal wave function; $\chi_{\mu_t}^{1/2}(\boldsymbol{\sigma}_p)\chi_0^0(\boldsymbol{\sigma}_1,\boldsymbol{\sigma}_2)$ the triton spin function (assuming $S=0$ for the neutrons); $\chi_{\mu_p}^{1/2}(\boldsymbol{\sigma}_p)$ the proton spin function; and $\psi_{M_i}^{J_i}$ and $\psi_{M_f}^{J_f}$ are the target and residual nuclear wave functions. Subscripts t, p, 1, 2 denote triton center-of-mass, proton, and neutron coordinates, respectively. $V(\mathbf{r}_p,\mathbf{r}_1,\mathbf{r}_2)$ is the interaction potential causing the transition, which we assume to be spin-independent. A two-nucleon "spectroscopic amplitude" is introduced by expanding the target nucleus wave function as a product of the states of the residual nucleus and states of the neutron pair:

$$\psi_{M_i}^{J_i}=\sum_{\substack{l_1 j_1, l_2 j_2 \\ L,\beta J_f}}(\beta J_f;[l_1 j_1, l_2 j_2]^L]\alpha J_i)[\psi^{\beta J_f}\psi^{l_1 j_1 l_2 j_2 L}(\mathbf{r}_1,\mathbf{r}_2,\boldsymbol{\sigma}_1\boldsymbol{\sigma}_2)]_{M_i}^{J_i}. \quad (9)$$

The bracket indicates angular-momentum coupling. The $\psi^{\beta J_f}$ are the states of the residual nucleus. The $\psi^{l_1 j_1 l_2 j_2 L}$ are the $S=0$ components of the antisymmetrized wave functions for the neutron pair in states $(l_i j_1)$ and $(l_2 j_2)$ coupled to total angular momentum L. The quantities $(\beta J_f;[l_1 j_1, l_2 j_2]^L]\alpha J_i)$ defined by Eq. (9) are generalized two-particle fractional parentage coefficients and contain the bulk of the nuclear structure information we wish to extract from the experiment.

Under certain restrictive assumptions or approximations to be discussed below, these "spectroscopic amplitudes" $(\beta J_f;[l_1 j_1, l_2 j_2]^L]\alpha J_i)$ can be factored out of the squared modulus in Eq. (8) to become the usual "spectroscopic factors" to be obtained by normalizing the theoretical cross section to the experimental value.

By inserting Eq. (9) into Eq. (8) and writing $\psi^{l_1 j_1 l_2 j_2 L}$ in terms of $L-S$ to $j-j$ transformation amplitudes, $((l_1\tfrac{1}{2})_{j_1}(l_2\tfrac{1}{2})_{j_2}|(l_1 l_2)_L(\tfrac{1}{2}\tfrac{1}{2})_0)_L$ and single-neutron orbitals, $\phi^{l_1}(\mathbf{r}_1)$, $\phi^{l_2}(\mathbf{r}_2)$, the sums over M_i, M_f, μ_t, μ_p, βJ_f, and

[19] A. K. Sen Gupta and D. M. Van Patter, Nucl. Phys. **50**, 17 (1964).
[20] We are indebted to J. R. Maxwell, who collaborated with us in this later work, for allowing us to include the Zn data in this paper.
[21] We are indebted to B. Bayman and E. Rost for the following theoretical discussion.

integration over the coordinates of the residual nucleus can be performed giving

$$\frac{d\sigma}{d\omega}=\frac{m_i m_f}{(2\pi\hbar^2)^2}\frac{k_f}{k_i}\sum_L\frac{1}{2L+1}\frac{n(n-1)}{2}\Big\{\sum_\mu\Big|\sum_{\substack{l_1j_1\\l_2j_2}}(\beta J_f;[l_1j_1,l_2j_2]^L]\alpha J_i)((l_1\tfrac{1}{2})_{j_1}(l_2\tfrac{1}{2})_{j_2}|(l_1l_2)_L(\tfrac{1}{2}\,\tfrac{1}{2})_0)_L$$

$$\times\int\phi_i^{(-)*}\left(\frac{\mathbf{r}_p+\mathbf{r}_1+\mathbf{r}_2}{3}\right)\Theta^*(\mathbf{r}_p,\mathbf{r}_1,\mathbf{r}_2)V(\mathbf{r}_p,\mathbf{r}_1,\mathbf{r}_2)[\phi^{l_1}(\mathbf{r}_1)\phi^{l_2}(\mathbf{r}_2)]_\mu{}^L\phi_p{}^{(+)}(\mathbf{r}_p)d^3r_1d^3r_2d^3r_p|^2\Big\}. \quad (10)$$

If the two neutrons are in nonequivalent orbitals, $(l_1j_1)\neq(l_2j_2)$, the term in the square brackets should be replaced by

$$\frac{1}{\sqrt{2}}\{[\phi^{l_1}(\mathbf{r}_1)\phi^{l_2}(\mathbf{r}_2)]_\mu{}^L+[\phi^{l_2}(\mathbf{r}_1)\phi^{l_1}(\mathbf{r}_2)]_\mu{}^L\}.$$

In Eq. (10), n is the total number of neutrons in the single-particle levels (l_1j_1) and (l_2j_2) included in the summation.

At present computer codes have not been written for doing the 9-dimensional integral of Eq. (10). Furthermore, progress is just now being made in developing 6-dimensional codes. However, several approximations are possible for reducing the above integral to a 3-dimensional problem which can be handled by modification of existing codes. The simplest such approximation is to assume a zero-range interaction between the proton and a point dineutron (point-triton approximation). With the point-triton approximation, the integral in Eq. (10) reduces to

$$\int\phi_i^{(-)*}(\mathbf{r})F_{Ll_1l_2}(r)Y_\mu{}^{L*}(\theta,\varphi)\phi_p{}^{(+)}(\mathbf{r})d^3r \quad (11)$$

where

$$F_{Ll_1l_2}(r)\propto\left(\frac{(2l_1+1)(2l_2+1)}{2L+1}\right)(l_1l_200|L0)[u_{n_1l_2}(r)u_{n_1l_2}(r)]. \quad (12)$$

The $u_{nl}(r)$ are the single-particle neutron radial wave functions.

In cases where the target and residual nuclei differ by a single pair of orbitals $(n_1l_1j_1)$ and $(n_2l_2j_2)$ we can factor Eq. (10) to isolate a "spectroscopic factor"

$$S_L(l_1j_1,l_2j_2)=\tfrac{1}{2}n(n-1)|(\beta J_f;[l_1j_1,l_2j_2]^L]\alpha J_i)|^2. \quad (13)$$

Under this very restrictive condition, Eq. (10) becomes, for the point triton assumption,

$$\frac{d\sigma}{d\omega}=\frac{m_i m_f}{(2\pi\hbar^2)^2}\frac{k_f}{k_i}\sum_L\frac{1}{2L+1}S_L(l_1j_1,l_2j_2)((l_1\tfrac{1}{2})_{j_1}(l_2\tfrac{1}{2})_{j_2}|(l_1l_2)_L(\tfrac{1}{2}\,\tfrac{1}{2})_0)_L{}^2\{\sum_\mu|\phi_i^{(-)*}(\mathbf{r})F_{Ll_1l_2}(r)Y_\mu{}^{L*}(\theta,\varphi)\phi_p{}^{(+)}(\mathbf{r})d^3r|^2\}. \quad (14)$$

If a model for the nuclear wave functions is available, the spectroscopic factor can be calculated from a relation which is equivalent to Eq. (13)

$$S_L(l_1j_1,l_2j_2)=\left[\langle 0|\psi^\dagger(\alpha J_iM_i)\left\{\frac{1}{(1+\delta_{j_1j_2})^{1/2}}[a_{l_1j_1}{}^\dagger a_{l_2j_2}{}^\dagger]^L\psi(\beta J_f)\right\}^{J_i}_{M_i}|0\rangle\right]^2, \quad (15)$$

where $\psi(\alpha J_i)|0\rangle$ and $\psi(\beta J_f)|0\rangle$ are normalized target and residual nuclear states, the $a_{lj}{}^\dagger$ are neutron creation operators for states (lj), and the brackets indicate angular momentum coupling. Thus the spectroscopic factor is the probability of finding in the target nucleus ground state, a given state of the residual nucleus plus two neutrons in states (l_1j_1) and (l_2j_2) coupled to angular momentum L. With S_L defined by Eqs. (13) or (15), Eq. (14) is of the form

$$d\sigma/d\omega=\textstyle\sum_L S_LG_L(\theta,k_i,k_f), \quad (16)$$

where G_L is independent of the structure of the nuclear states except for the neutron single-particle wave functions contained in F_L.

It should be noted again that the cross section can be written in the simple form of Eq. (16) only for the case in which the target and residual nuclei differ by a single pair of neutron states. If this is not the case, the Eq. (10) is of the form

$$\frac{d\sigma}{d\omega}=\sum_L\Big|\sum_{\substack{l_1j_1\\l_2j_2}}[S_L(l_1j_1,l_2j_2)]^{1/2}[G_L(\theta_1k_i,k_f,l_1j_1,l_2j_2)]^{1/2}\Big|^2. \quad (17)$$

In this case because of the coherence between the contribution from the various (lj) states, it is not, in general, possible to factor out a single spectroscopic factor for the reaction. This coherence can lead to collective effects in (p,t) reactions which have no analog in single-nucleon transfer reactions.

Since we do not yet have computer codes modified to use Eqs. (10) and (11) or (14), our analysis is based mainly on the use of Eq. (16) and the assumption that G_L is constant over the range of elements and Q values studied. The very close similarity of the angular distributions observed for a given L lends support to this assumption. We expect Eq. (16) to be a good approxima- for the elements Ti^{46} through Fe^{54} where the neutron configuration is expected to be nearly pure $(f_{7/2})^n$. The approximation of a pure j^n configuration or the degenerate configuration, discussed below, should be less valid in the region from $N=30$ to $N=40$ where the $2p_{3/2}$, $2p_{1/2}$ and $1f_{5/2}$ shells are filling. In this latter region, we have also compared the data with an approximate equation, derived from the pairing theory by Yoshida[22] which is of the form of Eq. (17).

Thus our procedure has been to take the experimental cross sections as being proportional to the spectroscopic factor. In practice it was possible to measure the (p,t) cross section only in the forward direction and hence our integrated cross sections are taken from $\theta_{\text{lab}}=10$ to 35°. The integrated cross sections for the $L=0$ and $L=2$ transitions studied are shown in Table II.

B. Plane-Wave Approximation

Several attempts were made to analyze the data using a plane-wave Butler code originally written for (p,d) reactions.[23] Because of the change in Q value and the change in atomic weight A the plane-wave predictions showed a variation of ± 3 degrees in the position of the principal maximum in the $L=0$ curves, even when a smooth radius variation with A was assumed. The relative spectroscopic factors obtained by normalizing the data to the same peak heights as the plane wave curves are shown in Table III and are seen to fluctuate wildly. The fluctuations were even greater if radii were chosen independently for each element to make the theoretical and experimental maxima coincide. Also, it was not possible to fit the $L=2$ transitions with the same radii as used for the $L=0$ transitions. At this point the plane-wave–Butler theory was abandoned and work is now in progress to use Eq. (14) for future analysis. Typical Butler fits are shown in Figs. 3 and 4.

TABLE III. Results of the PWBA-Butler analysis for the $L=0$ ground-state transitions. The cutoff radius has been obtained from the following expression: $r=1.7\ (A^{1/3}+3^{1/3})$ fermi.

Target nucleus	Ti^{48}	Fe^{54}	Fe^{56}	Ni^{58}	Ni^{60}	Cu^{63}	Cu^{65}
r (fermi)	8.63	8.88	8.96	9.03	9.11	9.21	9.29
Relative spectroscopic factor	27.0	1.03	11.5	1.70	8.56	11.1	43.5

C. Theoretical Spectroscopic Factors, Even-N Nuclei

1. *Seniority Coupling, j^n Configuration.*

The simplest model for calculating (p,t) spectroscopic factors is to neglect completely the protons and to assume that the neutrons in both the target and residual nuclear ground states are in the state of the lowest neutron seniority of the configuration j^n; that is, all neutron pairs are in the same state (lj), coupled to total angular momentum zero (and antisymmetrized). In addition, we assume that the excited states of the residual nucleus possess definite neutron seniority. Under this assumption, the spectroscopic factors for even-even nuclei as defined by Eqs. (13) or (15) are

$$S_0=\frac{n}{2}\frac{(2j+3-n)}{2j+1} \tag{18}$$

for the $L=0$ transition between states of zero neutron seniority, and

$$S_L=\frac{n(n-2)(2J_f+1)}{(2j-1)(2j+1)}=\frac{n(n-2)(2L+1)}{(2j-1)(2j+1)} \tag{19}$$

for the $L=J_f$ and $\Delta\nu_n=2$ transitions. For the odd-Z nuclei (but even N) the situation is more complicated. If we assume that the proton configuration does not change and that the neutrons in the target are in a state of seniority zero, Eq. (18) for the $\Delta\nu_n=0$ transitions is still valid. However, Eq. (19) must be modified to read

$$S_L=\frac{n(n-2)(2L+1)}{(2j-1)(2j+1)}\cdot\frac{(2J_f+1)}{(2j_p+1)(2L+1)} \tag{20}$$

since the strength for a given L is spread equally over the $(2j_p+1)(2L+1)$ magnetic substates of the state $\mathbf{J}_f=\mathbf{L}+\mathbf{j}_p$, where $\mathbf{j}_p$ is the total angular momentum of the protons. If the spectroscopic factors given by Eq. (20) for a given L are summed over the possible final states, J_f, the sum will have the same value as Eq. (19) for the even-even nuclei. This is a special case of a more general result to be expected on a pure core-excitation model[24] in which the excited states of odd-even nuclei are formed by coupling the odd particle to the states of the even-even core. In this case, the summed spectroscopic factors for the members of the odd-Z multiplet based on a given core state should equal the spectroscopic factor for excitation of the core state. Furthermore, the intensity ratios to the members of the odd-Z

[22] S. Yoshida, Nucl. Phys. **33**, 685 (1962).

[23] P. Gould, Nucl. Phys. **33**, 336 (1962). We wish to thank P. Gould for the plane wave calculations.

[24] See, for example, A. de Shalit, Phys. Rev. **122**, 1530 (1961).

core multiplet should follow the simple $(2J_f+1)$ rule. Any departure from these results will give a direct measure of the mixing of core states in the states of the odd-Z nucleus.

Returning to the simple neutron seniority spectroscopic factors, Eqs. (18) and (19) represent the probability that a pair of neutrons in the configuration j^n is coupled to a total orbital angular momentum L multiplied by the number of pairs. As a shell is filling the $L=0$ spectroscopic factor S_0 first increases linearly with n, reaches its maximum as the shell is half filled $(n=j+\frac{1}{2})$, and then decreases to the same value at the end of the shell as for $n=2$, reflecting the fact that the Pauli principle restricts the probability of a given pair being coupled to $J=0$, even though the seniority of the state is zero. The spectroscopic factors $S_L(L\neq 0)$ for $\Delta\nu_n=2$ increase approximately quadratically as n increases, to the end of the shell. In addition, $S_L=0$ $(L\neq 0)$ for $n=2$. Thus any $L\geq 2$ transition strength observed for nuclei with $n=2$ must come from neutron pickup from lower filled shells, or from admixtures of configurations other than j^n in the target ground state (see discussion below for $Ni^{58}(p,t)Ni^{56}$, for example.)

2. *Degenerate Configuration*

If several levels (l_1j_1), (l_2j_2), etc., are degenerate or nearly degenerate Eqs. (18) and (19) will be approximately correct if $(j+\frac{1}{2})$ is replaced by $\Omega=\frac{1}{2}\sum_{j_i}(2j_i+1)$, the total pair degeneracy of the levels. Eqs. (18) then becomes

$$S_0=\frac{n}{2}\frac{(2\Omega+2-n)}{2\Omega}. \tag{21}$$

In this approximation we are neglecting differences in the radial integrals and $LS-jj$ transformation amplitudes [Eq. (14)] for the various degenerate states. The equations derived from pairing theory (Sec. VC3 below) will reduce to Eq. (21) multiplied by 4Ω for the case of degenerate levels.

3. *Pairing theory.*

Yoshida[22] has derived expressions for the (p,t) cross sections in the pairing force approximation which should be appropriate for closed proton shell nuclei. He obtains for the spectroscopic amplitudes from each state (lj)

$$[S_0(lj)]^{1/2}=(2j+1)^{1/2}U_jV_j \tag{22}$$

for transitions between the zero quasiparticle ground states of even-even nuclei, and,

$$[S_L(l_1j_1,l_2j_2)]^{1/2}=-(2J_f+1)^{1/2}V_{j_1}V_{j_2} \tag{23}$$

for the transition from the zero quasiparticle ground state of the target to a two-quasiparticle state of the daughter nucleus with configuration (l_1j_1) (l_2j_2) and angular momentum $J_f=L$. The U_j's and V_j's are the occupation amplitudes of the states (lj) in the pairing theory and are defined in Ref. 25. The U_j refer to the daughter and the V_j to the target nucleus in Eqs. (22) and (23). Because of the coherence of contributions from the various paired configurations the spectroscopic amplitudes cannot, in general, be factored. However, Yoshida has shown, using a plane wave treatment of the two-neutron pickup reaction due to Newns[26] and an approximate expression for the radial integrals, that the $L=0$ cross section between ground states of even-even nuclei can be written

$$d\sigma/d\omega\propto j_0^2(QR)\left|\sum_j(2j+1)U_jV_j\right|^2 \tag{24}$$

which contains the spectroscopic amplitude of Eq. (22) multiplied by a factor $(2j+1)^{1/2}$ coming from the radial and angular integrals. We will refer loosely to the squared modulus in Eq. (24) as the "pairing spectroscopic factor," although strictly speaking it is not the spectroscopic factor defined by Eqs. (13) or (15). Yoshida's expression for the excitation of two quasiparticle states is more complicated and will not be given here.

Finally in the degenerate limit, if the constant pairing force matrix element approximation is made so that all of the V_j's are equal and are given by $V_j^2=n/2\Omega$ (parent nucleus) and $U_j^2=1-(n-2)/2\Omega$ (daugher nucleus), Eq. (24) reduces to

$$d\sigma/d\omega\propto j_0^2(QR)[n(2\Omega+2-n)]. \tag{25}$$

The expression in the bracket is just Eq. (21) multiplied by 4Ω. Equation (25) implies that the $L=0$, ground state cross sections will be proportional to Ω the total pair degeneracy, at the beginning and end of the shell $(n=2$ or $n=2\Omega)$ and approximately, to Ω^2 at midshell $(n=\Omega)$. This demonstrates the large collective enhancement possible in the (p,t) reaction due to the increase in effective degeneracy provided by residual interactions of the pairing force type.

In the sections that follow, we shall compare our data with Eqs. (18), (19), (24), and (25).

4. *Shell Model Calculations, $f_{7/2}$ Shell*

McCullen, Bayman, and Zamick[27] (hereafter referred to as MBZ) have performed an exact diagonalization of the energy matrix assuming a pure $(f_{7/2})^n$ configuration for neutrons and protons and using the methods of Talmi and co-workers.[28] The nucleon-nucleon interaction is taken from the spectrum of Sc^{42} and assumed to be charge independent. Thus the (p,t) spectroscopic factors calculated from the MBZ wave functions should be exact if their assumption of a pure $(f_{7/2})^n$ configuration and two-body forces is correct and if Coulomb

[25] S. Yoshida, Nucl. Phys. **38**, 380 (1962).
[26] H. C. Newns, Proc. Phys. Soc. (London) **76**, 489 (1960).
[27] J. D. McCullen, B. F. Bayman, and Larry Zamick, Phys. Rev. **134**, B515 (1964).
[28] See, for example, I. Talmi, Rev. Mod. Phys. **34**, 704 (1962).

effects can be neglected. Since the neutron-proton interaction is included, the states no longer have definite neutron seniority, except in the case of the calcium isotopes where the MBZ spectroscopic factors are then the same as those given in Sec. VC1. The comparison of the data with the MBZ spectroscopic factors is discussed in Sec. VIA.

VI. INTERPRETATION OF RESULTS

As mentioned in Sec. V, computer codes are not yet available for the realistic treatment of two-nucleon transfer reactions, even in the point triton approximation. Attempts at using existing plane-wave Born-approximation (PWBA) or DWBA codes, originally written for single nucleon transfer reactions, to extract meaningful spectroscopic factors from the data have failed. Thus, pending a more complete analysis, we have simply taken the integrated cross sections from 10 to 35 degrees for comparison with the theoretical spectroscopic factors. The integrated cross sections are shown in Table II and Figs. 28 through 31.

A. $f_{7/2}$ Shell Data

If a pure $(f_{7/2})^n$ configuration is assumed for neutrons and protons for the nuclei $Ti^{46,48,50}$, V^{51}, Cr^{52}, and Fe^{54}, the cross sections for a given L value can be expected to be directly proportional to the spectroscopic factors, defined by Eqs. (13) or (15), providing the dependence on Q value and target atomic weight can be neglected. Single-nucleon transfer data[29] indicate that the $(f_{7/2})^n$ configuration is a fair approximation for these nuclei.

The comparisons of the $L=0$, ground state, and lowest $L=2$ cross sections with the simple neutron seniority formulas [Eqs. (18) and (19)], as well as with the MBZ shell-model calculations, are shown in Table IV and Fig. 28. To provide an absolute normalization of the $f_{7/2}$ shell spectroscopic factors to the data we have also shown some recent results on the calcium isotopes which have been reported elsewhere.[30] The MBZ and neutron-seniority spectroscopic factors (which are the same for the calcium isotopes) have been normalized to the data at Ca^{44} for the $L=0$ points and at Ca^{48} for the $L=2$ points. The calculated $L=0$ spectroscopic factors are then a bit low for Ca^{42}, and too high for Ca^{48} but the over-all fit to the data is very satisfactory, giving us some confidence in our method of making a direct comparison between spectroscopic factors and cross sections.

TABLE IV. Ratio of lowest $L=0$ and $L=2$ integrated (p,t) cross sections to spectroscopic factors calculated by MBZ (Ref. 27) assuming pure $(f_{7/2})^n$ configuration. The ratios have been normalized to unity at Ca^{44} $(L=0)$ and Ca^{48} $(L=2)$.

Target nucleus	Ca^{42}	Ca^{44}	Ca^{48}	Ti^{46}	Ti^{48}	Ti^{50}	V^{51}	Cr^{52}	Fe^{54}
$L=0$	1.12	1	0.76	1.02	1.04	0.89	0.98	1.17	1.04
$L=2$	···	···	1	6.6	1.54	1.40	1.40	···	1.03

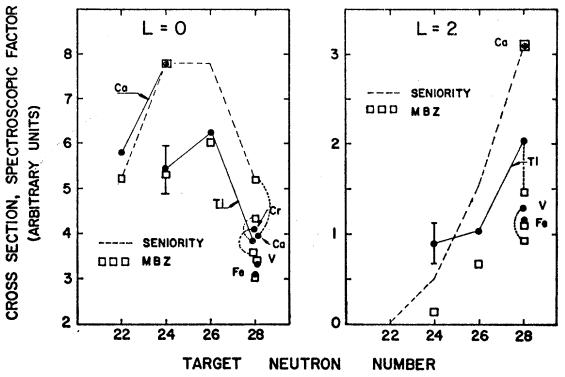

FIG. 28. Ground state, $L=0$, and first excited state, $L=2$, integrated cross sections (solid circles) and theoretical spectroscopic factors for $f_{7/2}$ shell nuclei. For V^{51} the lowest $L=2$ group is shown. Relative experimental errors are $\pm 10\%$ unless otherwise indicated. Theoretical spectroscopic factors (MBZ) are shown by open squares, connected to experimental points by dotted lines where uncertainties can arise. The dashed lines give the predictions of pure neutron seniority, normalized to the data at Ca^{44} $(L=0)$ and Ca^{48} $(L=2)$.

The effect of the protons in producing states of mixed neutron seniority is seen clearly in the reduction of the $L=0$ cross sections for the Ti isotopes below those of calcium. The relative cross sections for the $N=28$ isotone sequence agree fairly well with the MBZ calculation for Ti^{50}, V^{51} and Fe^{54} but not as well for Cr^{52} and Ca^{48}. All members of this sequence would show the same $L=0$ and $L=2$ strength in the simple neutron-seniority model.

With the normalization of the $L=2$ spectroscopic factors to the data at Ca^{48} (the only $L=2$ currently available for the calcium isotopes) the remaining $L=2$ predictions of MBZ are systematically too low, except for Fe^{54}. The discrepancy is especially great for Ti^{46}, indicating $2s$ or $1d$ hole admixtures in the $2+$ state of Ti^{44}, which could be excited by pickup of pairs in Ti^{46} from the $s-d$ shell, thereby increasing the $L=2$ cross section. The experimental situation is similar to that for the nickel isotopes which also show an excess of $L=2$ strength at the beginning of the shell relative to that predicted by the degenerate model (see below).

In the case of V^{51} our choice of the lowest $L=2$ theoretical spectroscopic factor is somewhat arbitrary since MBZ predict appreciable $L=2$ strength for states at 0.80 MeV ($\frac{3}{2}-$, 9.8%), 1.21 MeV ($11/2-$, 53%), 1.55 MeV ($\frac{5}{2}-$, 20%), and 1.58 MeV ($9/2-$, 17%), with spin, parity, and relative $L=2$ spectroscopic factor as given in the parentheses. We have lumped these four states together to obtain the theoretical $L=2$ point plotted in Fig. 28 since our resolution would not be

[29] E. Kashy and T. W. Conlon (to be published); J. C. Legg and E. Rost (to be published).

[30] G. Bassani, J. R. Maxwell, G. Reynolds, and Norton M. Hintz, to be published in the Proceedings of the Congrès International de Physique Nucléaires, Paris, 1964.

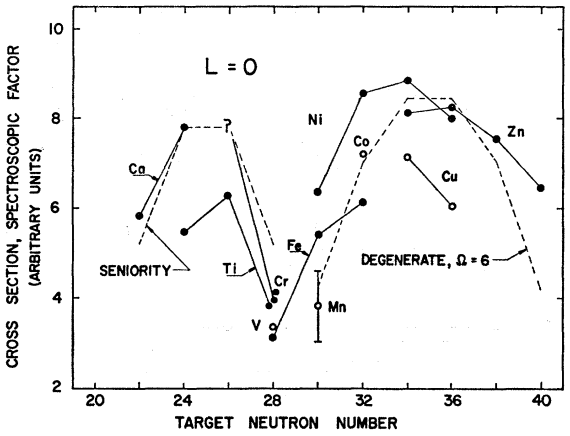

FIG. 29. Ground state, $L=0$, integrated cross sections (solid and open circles) and spectroscopic factors (dashed lines) for $f_{7/2}$ and $2p-1f_{5/2}$ shell nuclei. Odd-Z data are shown by open circles. Relative experimental errors are $\pm 10\%$ unless otherwise indicated.

sufficient to separate them. We see only a single $L=2$ peak at 1.0 MeV in the $V^{51}(p,t)V^{49}$ spectrum (Fig. 5). The remaining $L=2$ strength given by MBZ for this reaction occurs at 2.1 MeV and above and may account for some of the peaks which we see in this region.

Some confirmation of the predictions of the MBZ calculation comes from the absence ($\leq 10\%$) of an $L=2$ contribution to the ground states peak in $V^{51}(p,t)V^{49}$, which would be allowed by the selection rules [see Sec. IVC]. The only states predicted near zero energy in V^{49} by MBZ are the ground state ($\frac{7}{2}-$, 9.2%) and a state at 0.001 MeV ($\frac{5}{2}-$, 21.4%), where the spin, parity, and ratio of the predicted $L=2$ to the ground state $L=0$ spectroscopic factor is given in the parentheses. From the experimental cross sections for the Ca isotopes and the seniority spectroscopic factors, we can deduce a value for the integrated (10 to 35 degrees) ratio, G_0/G_2 of Eq. (16), of about 8. We would then expect $\leq 4\%$ of $L=2$ contribution to the ground-state group in the $V^{51}(p,t)V^{49}$ reaction, which is consistent with our observations.

Some qualitative comparisons can also be made between the spectra for $Ti^{48}(p,t)Ti^{46}$ and $V^{51}(p,t)V^{49}$ (Figs. 2 and 5) and the MBZ spectroscopic factors. For $Ti^{48}(p,t)Ti^{46}$ no appreciable ($\geq 8\%$ of the ground state) $L=0$ strength is predicted below 10 MeV and none is seen in the region surveyed. Aside from the first 2+ state in Ti^{46} at 0.89 MeV (which is calculated by MBZ to occur at 1.1 MeV), the only other state predicted to have appreciable $L=2$ strength ($\geq 10\%$ of the first 2+ state) is a state calculated to appear at 2.77 MeV with 67% of the first 2+ state $L=2$ strength. We see only a faint indication of (p,t) yield in this vicinity. The calculations of MBZ do predict a group of states in the vicinity of 3–4 MeV with strong $L=4$ and $L=6$ spectroscopic factors. The broad group we observe, peaked at ~ 3.7 MeV could correspond to these states.

Finally, for $V^{51}(p,t)V^{49}$, MBZ predict a $\frac{7}{2}-$ state at 2.88 MeV which should go mainly via an $L=0$ transition with $\sim 20\%$ of the ground state $L=0$ strength. We see no evidence for such a state. The failure to see the second $L=2$ state mentioned above in the reaction $Ti^{48}(p,t)T^{46}$, as well as the systematic $L=2$ discrepancy may indicate that the MBZ calculations are inadequate in obtaining the full "collective enhancements" of the first $L=2$ states within the assumption of a pure $(f_{7/2})^n$ configuration.

B. $2p$-$1f_{5/2}$ Shell Data

The lowest $L=0$ and $L=2$ integrated cross sections for nuclei in the $2p-1f_{5/2}$ shell are shown plotted in Figs. 29 and 30 together with the $f_{7/2}$ data for comparison. All of the data on these figures has the same normalization, although the theoretical curves are arbitrarily and differently normalized. The closing of the $f_{7/2}$ shell is shown clearly by the large dip at $N=28$ in the $L=0$ data and, less clearly, by the discontinuity in the $L=2$ data.

The $L=0$ data for the nickel isotopes also show the strong configuration mixing in the $2p-1f_{5/2}$ shell since the simple neutron seniority prediction of Eq. (18), if we assume only the $2p_{3/2}$ or the $1f_{5/2}$ shell is filling is in complete disagreement with the data. In fact, the gross features of the $2p-1f_{5/2}$ data can be reproduced assuming degeneracy of the $2p_{3/2}$, $2p_{1/2}$ and $1f_{5/2}$ levels and using Eq. 25 with $\Omega=6$ (dashed line or right side of Fig. 29). Some tendency for a shell closing at $N=40$ can be seen in the data for the nickel and zinc isotopes.

Also apparent from Fig. 29 is the reduction in the $L=0$ strengths in the odd-Z isotopes: V^{51}, Mn^{55}, Co^{59}, Cu^{63}, and Cu^{65}. This is presumably caused by admixtures to the ground states of configurations in which the neutrons are not coupled to seniority zero. For example, there could be present components of the type [(pro-

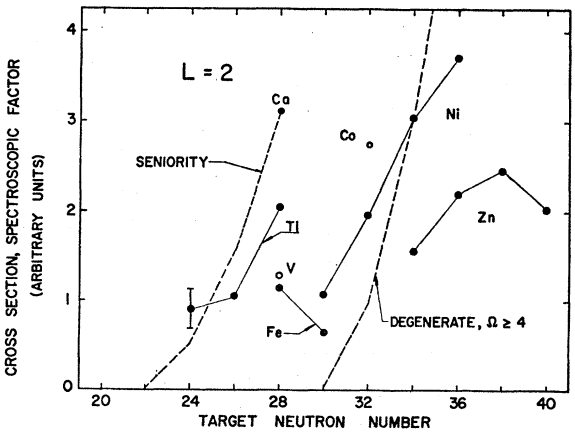

FIG. 30. First excited state, $L=2$, integrated cross sections for even nuclei (solid circles) ($f_{7/2}$ and $2p-1f_{5/2}$ shell). For the odd-Z nuclei, the lowest $L=2$ group is shown (open circles). Relative experimental errors are $\pm 10\%$ unless otherwise indicated. The dashed line shows the neutron seniority spectroscopic factor.

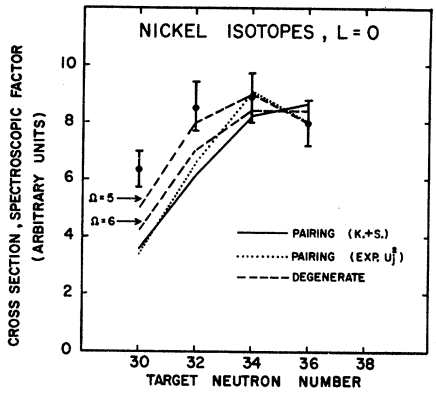

FIG. 31. Ground state, $L=0$ integrated cross sections for the nickel isotopes (points with error bars) and theoretical spectroscopic factors, arbitrarily normalized. The pairing spectroscopic factors are calculated from Eq. (24) using either theoretical U_j and V_j from Ref. 31 (solid line) or experimental U_j^2 from Ref. 32 (dotted line), Also shown are the predictions of the degenerate model, Eq. (25), with $\Omega=5$ and $\Omega=6$ (dashed lines).

tons)$_{3/2-}$ (neutrons)$_{2+}]_{3/2-}$ in the copper isotopes. Admixtures of this type, if sufficiently strong, would produce $L=2$ contributions to the ground state transitions. These are not seen experimentally (see Secs. IVC, G, and J). However, $L=2$ cross sections are expected to be reduced by about a factor of 8 from $L=0$ cross sections with the same spectroscopic factor, corresponding to the ratio, G_0/G_2 of Eq. (16) (see Sec. VIA). Complete shell-model calculations for the $2p-1f_{5/2}$ shell would be highly desirable.

The effect of opening the closed $f_{7/2}$ proton shell can be seen in the reduction of the $L=0$ cross sections for the iron isotopes below that for the nickel isotopes with the same neutron number. This effect could be due either to admixtures of the type [(protons)$_{2+}$ (neutrons)$_{2+}]_{0+}$ in the ground states of the iron isotopes, or to a reduction of the effective degeneracy in the $2p-1f_{5/2}$ shell [see remarks after Eq. (25)] caused by a repulsion upward of the $f_{5/2}$ neutron level by the $f_{7/2}$ proton holes.

The zinc isotopes, which have two protons added beyond the $f_{7/2}$ shell, show at first a reduction, then an increase in their $L=0$ cross sections relative to those for the nickel isotopes with the same neutron number. Both effects mentioned above could be operating, with the effect of the 2+ proton configuration admixture dominating for Zn^{64}, but with the effect of an increasing degeneracy, presumably from the $1g_{9/2}$ shell, predominating as the neutron number increases.

The ground state $L=0$ data for the nickel isotopes can also be compared with the "paring spectroscopic factor" [Eq. (24)], using theoretical U_j and V_j from the work of Kisslinger and Sorensen.[31] The relative cross sections predicted by pairing theory with the Yoshida formula are shown in Fig. 31 (solid line) along with those calculated using experimental U_j^2 from single nucleon transfer experiments[32] (dotted curve) and those from the degenerate model [Eq. (25)] with $\Omega=5$ and $\Omega=6$ (dashed lines). The theoretical curves have been arbitrarily normalized to agree with the data at the average of the Ni^{62} and Ni^{64} points. All three calculations are in approximate agreement with the data, the degenerate curve with $\Omega=5$ being the best fit. The theoretical curves show too rapid a rise with increasing neutron member as compared to experiment. This comparison emphasizes the urgent need to obtain *absolute* (p,t) spectroscopic factors through use of reliable DWBA calculations. An excess of $L=0$ strength at the beginning of the shell would indicate the presence, in the ground states, of pairs from the lower shells, which becomes relatively less important as the $2p-1f_{5/2}$ shell fills, while a decrease relative to theory at higher neutron numbers would indicate the increasing presence of "quadrupole fluctuations" or four quasiparticle excitations in the ground state, thus decreasing the number of zero coupled pairs. The latter would also imply an increase of the $L=2$ strength relative to the simple degenerate model which seems not to be present (see Fig. 30). The increased $L=2$ strength, however, might not all lead to the first 2+ state. More data on excited states of the nickel isotopes is needed to resolve this question. Finally, it should be mentioned that the absolute "pairing spectroscopic factors" predicted with the experimental single-nucleon transfer occupation members were about a factor of 1.5 lower than those calculated from the Kisslinger and Sorenson values, reflecting the fact that a relatively small occupation of the $g_{9/2}$ level ($V_j^2\sim 1-2\%$ as predicted by pairing theory) can contribute significantly to the (p,t) cross section since the U_j and V_j enter linearly into Eq. (24). Single-nucleon transfer reactions are much less sensitive to small configuration admixtures since they measure U_j^2 or V_j^2. In the case of the $g_{9/2}$ shell the single-nucleon transfer data are consistent with $V_j^2=0$. Again the need for absolute experimental spectroscopic factors is seen.

The lowest $L=2$ integrated cross sections for both the $1f_{7/2}$ and $2p-1f_{5/2}$ shell are shown in Fig. 30 along with the predictions of Eq. (19) for seniority coupling of the neutrons (dashed lines). Since the shape of the curve predicted by Eq. (19) does not depend on j, the equation should be approximately correct for the degenerate case as well. The rapid rise of the $L=2$ cross sections for the nickel isotopes, as the shell is filling, is in qualitative agreement with seniority spectroscopic factors. However, the rise in the data is considerably less pronounced than in the theory, again leaving some doubt as to the interpretation of the discrepancy because of the lack of absolute spectroscopic factors.

The relatively large value for the Ni^{58} cross section to the first 2+ state in Ni^{56} shows either the presence of extra pairs in the $2p-1f_{5/2}$ shell in the ground state of

[31] L. S. Kisslinger and R. A. Sorensen, Kgl. Danske Videnskab. Selskab, Mat. Fys. Medd. **32**, No. 9 (1960).

[32] R. H. Fulmer and A. L. McCarthy, Phys. Rev. **131**, 2133 (1963). R. H. Fulmer, A. L. McCarthy, and B. L. Cohen, and R. Middleton, Phys. Rev. **133**, B955 (1964).

Ni^{58}, as mentioned above, or contributions to the cross section from pickup of pairs from the $f_{7/2}$ shell, if we assume that the 2+ state has been reached by pickup of two neutrons from the same single particle state. An alternate explanation, discussed in Sec. IVH, is that the 2+ state in Ni^{56} consists mainly of an $f_{7/2}$ hole and a $2p_{3/2}$ or $f_{5/2}$ particle, which could then be reached by pair pickup from the ground state of Ni^{58} with a normal shell-model configuration.

The low (relative to nickel) cross sections for the lowest $L=2$ transitions in the zinc isotopes are somewhat surprising since the addition of two protons would be expected to produce more $L=2$ coupled pairs in the Zn ground states. Evidently the additional $L=2$ strength is going to higher 2+ states. There is some indication of this in the case of $Zn^{66}(p,t)Zn^{64}$ where a strong state is seen at 2.7 MeV which may be mainly $L=2$ (see Fig. 27). A similar explanation may hold for the Fe^{56}, $L=2$ point. Further work is in progress on the excited spectra of the nickel and zinc isotopes to resolve this question.

The high cross section for the first $L=2$ group in $Co^{59}(p,t)Co^{57}$ may reflect the additional $L=2$ component in the neutron wave function made possible by the presence of the odd proton, as discussed above. Unfortunately, we have at present no data for the $L=2$ transitions in the copper isotopes.

VII. CONCLUSIONS

The (p,t) reaction, and other two nucleon transfer reactions, can give information on the angular momentum coupling of pairs and on correlations in the occupation of single particle states not easily obtained in other ways. The (p,t) reaction can also be very useful in reaching otherwise inaccessible nuclei and in assigning spins and parities because of its simple selection rules.

The generally good agreement obtained in comparing $L=0$ integrated cross sections with two-nucleon spectroscopic factors, calculated from appropriate models, is strong evidence that the reaction proceeds by a direct pickup of a neutron pair. Moreover, the Q and A dependence of the reaction mechanism, which is given by the factor G_L Eq. (16), seems to be weak.

The predominance of the ground state, or lowest $L=0$ transition, shows the highly pair-correlated nature of this state. A tendency is also seen for the bulk of the $L=2$ strength to go to the first 2+ state in even-even nuclei, or to states in odd-Z nuclei with approximately the same excitation energy, as would be predicted by a core-excitation model.

In the $f_{7/2}$ shell, the $L=0$ ground state strengths are in much better agreement with the "exact" shell-model calculations of MBZ than with the results predicted by simple neutron seniority. The agreement with the MBZ spectroscopic factors is less satisfactory for the lowest $L=2$ transitions; the theory systematically underestimates the $L=2$ strength. Since the MBZ calculations also generally overestimate the energy of the first 2+ state and underestimate its $B(E2)$ value, the conclusion is that the assumed $(f_{7/2})^n$ configuration is inadequate to account for the "collective" properties of these states although the ground states are well described by this simple configuration. More detailed studies in the $f_{7/2}$ shell are planned when better resolution is available to check the transition strengths to the many $(f_{7/2})^n$ levels predicted by MBZ.

Appreciable configuration mixing in the $2p-1f_{5/2}-1g_{9/2}$ shell is evidenced by the need for $\Omega=6$ in the degenerate model [Eq. (25)] for the $L=0$ transitions. The predictions of the pairing theory for the $L=0$ transitions in the nickel isotopes, using either theoretical U_j and V_j calculated by Kisslinger and Sorensen or experimental values deduced from single-nucleon transfer experiments, are only in qualitative agreement with experiment. The reason for the discrepancy is not clear since calculations are not available in which the DWBA overlap integrals of Eq. (10) are treated realistically. Q-value effects are expected to be even more troublesome in two-nucleon than in single-nucleon transfer theories since a product of two single-particle bound states appears in the radial integral for the former. The data in both the $f_{7/2}$ and the $2p-1f_{5/2}$ shells does seem to indicate the presence of extra pairs, from lower shells, in the ground states near the beginning of each shell. The discrepancy between the $L=0$ data and pairing theory for the $2p-1f_{5/2}$ shell could thus be due either to this effect or to an overestimate of the contribution of $1g_{9/2}$ pairs to the cross section.

The behavior of the $L=2$ cross sections in the $2p-1f_{5/2}$ region, especially that of the nickel isotopes, indicates that the first 2+ states are not very pure in seniority. Calculations of $L=2$ spectroscopic factors for these states, using the pairing theory with quadrupole forces, would be highly desirable.

Finally, reliable DWBA calculations, including if possible finite range effects, are needed to remove uncertainties in our interpretations due to lack of knowledge of absolute experimental spectroscopic factors.

ACKNOWLEDGMENTS

We are indebted to Dr. Peter Gould for a thorough study of the use of the PWBA and existing DWBA approximations in fitting our data. Many of our ideas on the interpretation of the (p,t) reaction came from discussions with Professor Ben Bayman and Professor B. R. Mottelson. We also wish to thank Dr. J. R. Maxwell for help on the later phases of this experiment and for the use of his data on the zinc isotopes prior to publication. Finally, we wish to thank F. Becchetti, J. Benjamin, M. Fricke, D. Madland, G. Reynolds, and L. Williams for their help in data taking and analysis.